

# Impact of Weather Conditions on Generalized Frequency Division Multiplexing over Gamma Gamma Channel

Muhammad Sameer Ahmed, Piotr Remlein, Tansal Gucluoglu

**Abstract**—The technique called as Generalized frequency division multiplexing (GFDM) used in the free space optical channel can be a good option for implementation free space optical communication systems. This technique has several strengths e.g. good spectral efficiency, low peak-to-average power ratio (PAPR), adaptability and low co-channel interference. In this paper, the impact of weather conditions such as haze, rain and fog on GFDM over the gamma-gamma channel model is discussed. A Trade off between link distance and system performance under intense weather conditions is also analysed. The symbol error probability (SEP) of GFDM over the gamma-gamma turbulence channel is derived and verified with the computer simulations.

**Keywords**—Free space optics, generalized frequency division multiplexing, weather conditions, gamma gamma distribution.

## I. INTRODUCTION

**F**REE space optical (FSO) communications are under intense study due to their advantages including larger bandwidth, lower power consumption, higher transmission rates, and better security over radio frequency (RF) communications [1], [2]. FSO links are recognized as a fundamental part of the development of future wireless networks, since they can improve the system capacity [3]. On the other hand, atmospheric attenuation and turbulence due to changes in refractivity are the disadvantages of FSO which may lead to the severe signal distortions [4].

In the literature, there are several channel models proposed to represent the random behaviour of FSO links [5] to analyze the performance of wireless systems. Gamma-Gamma (GG) distribution [6] is a product of two random variables for large scale and small scale optical wave fluctuations which can model moderate to strong turbulence levels. Since it is a generalized model including K-distribution and negative exponential, it is widely used in the literature. The GG channel model is studied by [7], in which modelling of an orthogonal frequency division multiplexing (OFDM) based RF-FSO system with weather condition of Bhubaneswar city is analyzed. In [8], the GG channel with a coherent transceiver system is evaluated in terrestrial FSO under haze, rain, and fog weather conditions. Similarly, the performance of a GG channel - based OFDM-FSO model is also investigated

under diverse weather conditions [9]. OFDM transmission over FSO links is one of the special cases of Multiple subcarrier modulation (MSM) discussed in [10], [11] where the bit stream is first mapped into OFDM symbols and then modulated over independent subcarriers at different frequencies with the use of the intensity modulation direct detection (IM/DD) technique. The main drawbacks of OFDM in MSM schemes are unfavorable high peak-to-average power ratios (PAPR) [12] due to the optical power inefficiency and frequency synchronization is another issue to preserve the orthogonality. In order to overcome the limitations of OFDM, generalized frequency division multiplexing (GFDM) has been proposed [13].

GFDM is a flexible multicarrier modulation scheme [14] with some advantages over OFDM. GFDM has a single cyclic prefix (CP) part for the entire block, which makes it spectrally more efficient than OFDM, as CP has to be inserted after every OFDM symbol. The number of subsymbols per subcarrier can be altered in a GFDM block to transmit more symbols in one GFDM block, whereas in OFDM have single subsymbol per each subcarrier [16]. Circular properties of the signal are preserved over time and frequency domains by a digital filter [15]. This process reduces out of band (OOB) emissions and PAPR compared to OFDM [14], which lowers the adjacent channel interference and the constraints on power amplifiers [16], [17]. GFDM block structure can be shaped as desired to match the limitations of real-time applications by reducing the signal length [16]. Algorithms developed for OFDM and MIMO techniques can be easily adopted to GFDM as discussed in [16] and [18]. However, there is no previous work investigating GFDM transmission over any FSO links.

The remainder of this paper is organized as follows: Section II presents the GFDM system model over the GG distribution. Performance analysis is discussed in Section III. Section IV discusses the Simulation results. Concluding remarks are given in Section V.

## II. SYSTEM MODEL

In multicarrier transmission schemes, narrowband subcarriers are used to transmit data simultaneously. A GFDM block consists of  $K$  subcarriers and  $M$  subsymbols. The total number of symbols in one block is given by  $N = KM$ , Fig. 1. In the system model, a data source provides binary data to a mapper (QAM) which maps the bits into symbols by  $2^\mu$ -valued complex constellation where  $\mu$  is

M. S. Ahmed is with the Department of Electronics and Communication Engineering, Yildiz Technical University, Istanbul, Turkey (e-mail: samahmed1890@gmail.com).

P. Remlein is with the Poznan University of Technology, Poznan, Poland (e-mail: piotr.remlein@put.poznan.pl).

T. Gucluoglu is with the Yildiz Technical University, Istanbul, Turkey (e-mail: tansal@yildiz.edu.tr).

the modulation order. After mapping, a vector is obtained which represents a data symbol block that contains the total number of  $N$  elements which can further be decomposed into  $M$  subsymbols and it can be denoted as

$$s_{k,m} = [s_{0,0}, s_{1,0}, s_{K-1,0}, \dots, s_{K-1,M-1}]^T. \quad (1)$$

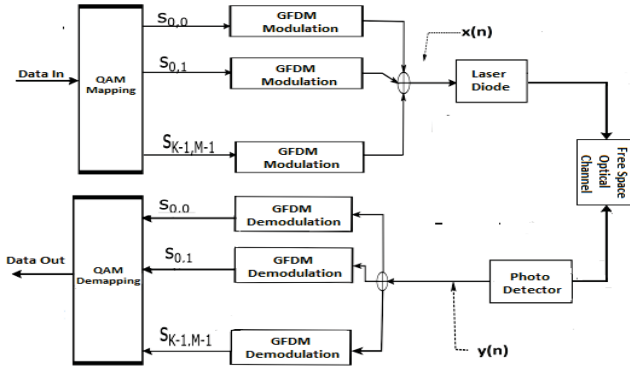


Fig. 1 System model for GFDM-FSO

The real GFDM signal can be obtained by enforcing Hermitian symmetry before the IFFT block in GFDM modulation, so that each piece of data after QAM mapping is arranged symmetrically, as shown in [19]. Then the GFDM symbols are obtained by up-sampling the data symbols and circularly convolved them with filter  $g(n)$ . After that they are up converted to the corresponding subcarrier frequency. Finally, the superposition of all symbols leads to the GFDM signal [20]. An Intensity modulation with direct detection (IM/DD) scheme can be used for transmitting GFDM over FSO channel which requires only real and positive RF signals. This approach with real value IFFT output after using Hermitian symmetry is also discussed in [11]. A GFDM signal with IM/DD can be written as

$$x(n) = \sum_{m=0}^{M-1} \sum_{k=0}^{K-1} s_{k,m} g_m(n - MK) e^{j2\pi \frac{k}{K} n}, \quad (2)$$

where  $n = \frac{K}{T_s} t$ ,  $s_{k,m}$  are the complex symbols over  $k^{th}$  subcarrier and  $m^{th}$  subsymbols. Let  $y(n)$  be the received signal for the transmitted signal  $x(n)$  which passes through the GG channel. Assuming perfect reception at the photo detector [21].

$$y(n) = \rho \cdot x(n) \cdot h + w(n) \quad (3)$$

where  $w(n)$  represents the AWGN sample,  $\rho$  is the photo detector responsivity which is assumed to be unity [19] and

$$h = h_g h_a \quad (4)$$

where  $h_a$  is the deterministic path loss that can be described by the Beer-Lambert law

$$h_a = \exp(-\xi L), \quad (5)$$

where  $\xi$  is the attenuation coefficient in dB/km which is calculated by various models [8] and  $LD$  is the link distance in km.

Fog is the most severe effect that dominates atmospheric attenuation due to the particle size of fog. The equation below

defines the specific attenuation of fog given by a common empirical model [8].

$$\xi_{fog} = \frac{3.91}{V} \left( \frac{\lambda}{550} \right)^q, \quad (6)$$

where  $V$  is the visibility in km and  $\lambda$  is the wavelength in nm. and  $q$  is the particle size distribution coefficient of scattering.

According to the Kim model,  $q$  is given as

$$\begin{aligned} q &= 1.6 & (V > 50km) \\ &= 1.3 & (6km < V < 50km) \\ &= 0.16V + 0.34 & (1km < V < 6km) \\ &= V0.5 & (0.5km < V < 1km) \\ &= 0 & (V < 0.5km) \end{aligned} \quad (7)$$

Rain has a distance-reducing impact on FSO, although its impact is significantly lower than that of fog. The attenuation caused by the rain for FSO can be well approximated by the empirical formula given below

$$\xi_{rain} = \frac{2.9}{V} \quad (8)$$

and  $h_g$  denotes the variations of the fading with a GG distributed PDF shown below, [6], [22]

$$p_{h_g}(h_g) = \frac{2(\alpha\beta)^{\frac{\alpha+\beta}{2}}}{\gamma(\alpha)\gamma(\beta)} h_g^{\frac{\alpha+\beta}{2}-1} K_{\alpha-\beta}(2\sqrt{\alpha\beta h_g}), \quad (9)$$

where  $\alpha$  and  $\beta$  parameters are the large scale and small scale optical wave intensity scintillation [22] and defined for spherical wave [11] by (5) and (6).  $K(\cdot)$  is the Bessel function of the second order and  $\gamma(\cdot)$  is the Gamma function.

$$\alpha = \left[ \exp \left\{ \frac{0.49\sigma^2}{(1 + 0.18d^2 + 0.56\sigma^{\frac{12}{5}})^{\frac{7}{6}}} \right\} - 1 \right]^{-1}, \quad (10)$$

$$\beta = \left[ \exp \left\{ \frac{0.51\sigma^2(1 + 0.69\sigma^{\frac{12}{5}})^{-5/6}}{(1 + 0.9d^2 + 0.62d^2\sigma^{\frac{12}{5}})^{\frac{7}{6}}} \right\} - 1 \right]^{-1}, \quad (11)$$

where  $\sigma^2 = 0.5C_n^2 k^{7/6} L^{11/6}$  is the Rytov variance for spherical wave propagation [26] and  $d = \sqrt{\pi D^2 / 2\lambda L}$ ,  $D$  = the diameter of the receiver lens aperture,  $L$  = link distance.  $\lambda$  = wavelength.  $k = 2\pi/\lambda$ , and  $C_n^2$  = structure constant of the refractive index. GG distribution is a more general model which includes the result of the K-distribution model when ( $\beta = 1$ ).

Once the signal is received at the photo detector, the demodulation of the GFDM signal is obtained by the match filter and the zero force filter (ZF) proposed by [27]. The joint PDF of the free space optical channel can be computed by

$$f_h(h) = \left| \frac{d}{dh} \left( \frac{h}{h_a} \right) \right| \cdot f_{h_g} \left( \frac{h}{h_a} \right) \quad (12)$$

$$\left| \frac{d}{dh} \left( \frac{h}{h_a} \right) \right| = \frac{1}{a} \quad (13)$$

and

$$f_{h_g} \left( \frac{h}{h_a} \right) = \frac{2(\alpha\beta)^{\frac{\alpha+\beta}{2}}}{\gamma(\alpha)\gamma(\beta)h_a^{\frac{\alpha+\beta}{2}-1}} h_g^{\frac{\alpha+\beta}{2}-1} K_{\alpha-\beta} \left( 2\sqrt{\frac{\alpha\beta h_g}{h_a}} \right) \quad (14)$$

When we put (13) and (14) in (12)

$$f(h) = \frac{2(\alpha\beta)^{\frac{\alpha+\beta}{2}}}{\gamma(\alpha)\gamma(\beta)h_a^{\frac{\alpha+\beta}{2}}} h_g^{\frac{\alpha+\beta}{2}-1} K_{\alpha-\beta} \left( 2\sqrt{\frac{\alpha\beta h_g}{h_a}} \right) \quad (15)$$

$$K_n(z) = \frac{1}{2} G_{0,2}^{2,0} \left[ \frac{z^2}{4} \right]_{n/2, -n/2}^{-, -} \quad (16)$$

After using the above equation, (8) can be shown in terms of the Meijer G function [11]

$$f(h) = \frac{2(\alpha\beta)^{\frac{\alpha+\beta}{2}}}{\gamma(\alpha)\gamma(\beta)h_a^{\frac{\alpha+\beta}{2}}} h_g^{\frac{\alpha+\beta}{2}-1} G_{0,2}^{2,0} \left[ \frac{\alpha\beta h_g}{h_a} \right]_{\frac{\alpha-\beta}{2}, \frac{\beta-\alpha}{2}}^{-, -} \quad (17)$$

### III. PERFORMANCE ANALYSIS

It is necessary to evaluate the degradation which occurs in an FSO link carrying GFDM signals due to atmospheric turbulence, by determining the closed form expression of symbol error probability (SEP). SEP for QAM-GFDM is given by [24]

$$P_{s,n}(e) = 2 \left( \frac{p-1}{p} \right) \operatorname{erfc}(\sqrt{\gamma}) - \left( \frac{p-1}{p} \right)^2 \operatorname{erfc}^2(\sqrt{\gamma}), \quad (18)$$

where  $p = \sqrt{2\mu}$  and  $\gamma$  represent instantaneous SNR and are shown as

$$\gamma = \bar{\gamma} h_g^2, \quad (19)$$

where  $\bar{\gamma}$  is the equivalent SNR explained in [25]. SEP of GFDM over a GG turbulence channel can be computed by the following equation

$$P_e = \int_0^\infty P_{s,n}(e) f(h) dh_g. \quad (20)$$

Since the derivation is lengthy, we resort to simulation results to find out the impact of weather conditions on the system performance.

### IV. SIMULATION RESULTS

In this section, performance in terms of symbol error probability (SEP) has been plotted. The impact of weather conditions (such as haze, rain, fog) on GFDM over a GG channel is analysed. The number of subcarriers  $K = 128$  and the number of subsymbols  $M = 5$ , and the roll-off factor of 0.5 have been chosen. 16 QAM signalling has been selected. The  $\alpha = 4.19$  and  $\beta = 2.27$  parameters are selected for a moderate turbulence level. The attenuation coefficient values have been shown for different weather conditions in Table I [23].

In Fig. 2, SEP of low rain has been compared over different values of link distance ( $LD$ ) obtained from the set of values (0.5, 1, 1.5, 2, 2.5) in km. Attenuation coefficient  $\xi = 6.27$  in dB/km has been selected for the analysis. At  $LD = 2.5$  and  $0.5$  km, SEP is computed as  $6.01 \times 10^{-5}$  and  $9 \times 10^{-3}$ , respectively. Clearly, increasing the distance between

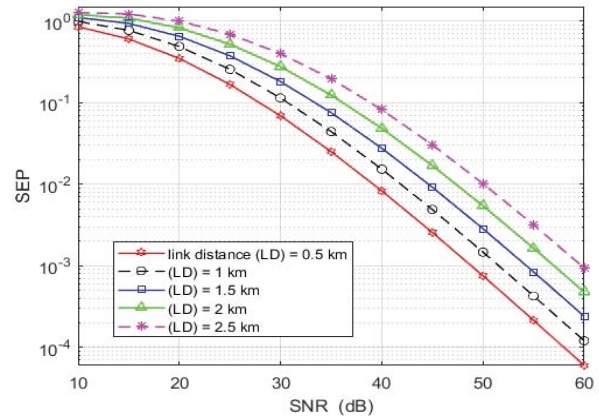


Fig. 2 Performance analysis at low rain

TABLE I  
ATTENUATION COEFFICIENT VALUES FOR DIFFERENT WEATHER CONDITIONS

Attenuation coefficient in dB/km		
Weather	Low	Medium
Haze	1.537	4.28
Rain	6.27	9.64
Fog	15.55	33.961

the transmitter and receiver will have a decreasing impact on the performance.

The Comparison that has been discussed in Fig. 3 between various weather conditions and clear weather means there is no weather effect on the system. Table I is used to illustrate different weather conditions. The parameter  $LD = 1\text{ km}$  has been chosen for all the conditions. Obviously the performance in clear weather is better than the performance in other weather conditions, especially in medium fog.

In Fig. 4, a trade off between link distance and performance is discussed when the attenuation coefficient increases. Generally, in intense weather conditions the performance decreases, especially in fog and snow, etc. The Fog case has been chosen for discussion. In order to have better

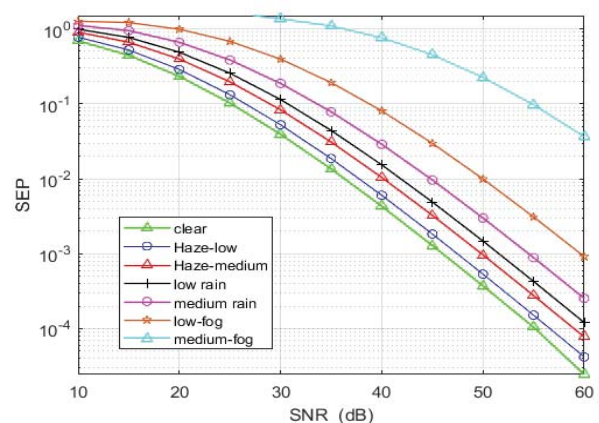


Fig. 3 Comparison between impact of different weather conditions with the clear weather at  $LD = 1\text{ km}$



performance, a decrease in link distance is chosen, i.e., short distance transmission is considered. As shown in Fig. 3, SEP at 250 m is  $7.11 \times 10^{-5}$  and it decreases to  $2.0 \times 10^{-3}$  at 1.25 km. Almost the same performance can be obtained in the rain over the distance of 2.5 km, as discussed in Fig. 1.

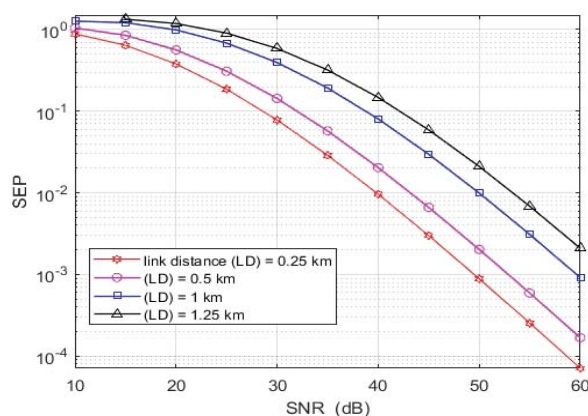


Fig. 4 Impact of fog on different values of link distance

## V. CONCLUSION

The performance of GFDM over a GG channel is analyzed with the impact of different weather conditions, such as haze, rain and fog. In this paper, performance analysis has been investigated in terms of SEP. The results demonstrate that the performance of the system in clear weather obviously outperforms the system impacted by weather. One can choose a shorter link distance in order to increase the performance during intense weather conditions.

## REFERENCES

- [1] GM. A. Khalighi, M. Uysal, Survey on free space optical communication: A communication theory perspective, *IEEE Communications Surveys and Tutorials*, 16(4), pp. 2231-2258, 2014.
- [2] Z. Ghassemloo, S. Arnon, M. Uysal, Z. Xu, J. Cheng, Emerging Optical Wireless Communications-Advances and Challenges, *IEEE Journal on Selected Areas in Communications*, 33(9), pp. 1738-1749, 2015.
- [3] J. Perez, F. I. Chicharro, B. Ortega, J. Mora, On the evaluation of an optical OFDM radio over FSO system with IM-DD for high-speed indoor communications, in: *International Conference on Transparent Optical Networks*, pp. 14, 2017.
- [4] H. Kaushal, G. Kaddoum, Optical Communication in Space: Challenges and Mitigation Techniques, *IEEE Communications Surveys and Tutorials*, 19(1), pp. 5796, 2017.
- [5] K. Anbarasi, C. Hemanth, R. Sangeetha, A review on channel models in free space optical communication systems, *Optics & Laser Technology*, 97, pp. 161-171, 2017.
- [6] R. Gupta, T. Singh Kamal, P. Singh, Concatenated LDPC-TCM Codes for Better Performance of OFDM-FSO System Using Gamma Gamma Fading Model, *Wireless Personal Communications*, 106(8), pp. 2247-2260, 2019.
- [7] Prabu K, P. S. Pati, Modeling of OFDM based RoFSO system for Bhubaneswar weather conditions, *Wireless Personal Communications*, May (2019), pp. 121, 2019.
- [8] D. Kakatia, S. C. Arya, Performance of 120 Gbps Single Channel Coherent DP-16-QAM in Terrestrial FSO Link under Different Weather Conditions, *Optik*, 178, pp. 1230-1239, 2019.
- [9] M. Sultana, A. Barua, J. Akhtar, M. I. Reja, Performance Investigation of OFDM-FSO System under Diverse Weather Conditions of Bangladesh, *International Journal of Electrical and Computer Engineering*, 8(5), pp. 3722-3731, 2018.

- [10] H. Rongqing, Z. Benyuan, H. Renxiang, T. A. Christopher, R. D. Kenneth, R. Douglas, Subcarrier multiplexing for high-speed optical transmission, *Journal of Lightwave Technology*, 20(3), pp. 417-424, 2002.
- [11] A. Bekkali, C. B. Naila, K. Kazaura, K. Wakamori, M. Matsumoto, Trans-mission analysis of OFDM-based wireless services over turbulent radio-on-FSO links modeled by Gamma - Gamma distribution, *IEEE Photonics Journal*, 2(3), pp. 510-520, 2010.
- [12] J. Armstrong, Peak-to-average power reduction for OFDM by repeated clipping and frequency domain filtering, *Electronics Letters*, 38(5), p. 246, 2002.
- [13] R. Gerzaguet, N. Bartzoudis, L. G. Baltar, V. Berg, J. B. Dore, D. Ktenas, O. Font-Bach, X. Mestre, M. Payaro, M. Farber, K. Roth, The 5G candidate waveform race: a comparison of complexity and performance, *Eurasip Journal on Wireless Communications and Networking*, 13, Springer Open, 2017.
- [14] G. Fettweis, M. Krondorf, S. Bittner, GFDM - generalized frequency division multiplexing, *IEEE Vehicular Technology Conference*, pp. 14, 2009.
- [15] N. Michailow, S. Krone, M. Lentmaier, G. Fettweis, Bit error rate performance of generalized frequency division multiplexing, *IEEE Vehicular Technology Conference*, pp. 15, 2012.
- [16] N. Michailow, M. Matthe, I. S. Gaspar, A. N. Caldevilla, L. L. Mendes, A. Festag, G. Fettweis, Generalized frequency division multiplexing for 5th generation cellular networks, *IEEE Transactions on Communications*, 62(9), pp. 3045-3061, 2014.
- [17] S. K. Antapurkar, A. Pandey, K. K. Gupta, GFDM performance in terms of BER, PAPR and OOB and comparison to OFDM system, *IEEE AIP Conference Proceedings*, pp. 16, 2016.
- [18] W. D. Dias, L. L. Mendes, J. J. P. C. Rodrigues, Low complexity GFDM receiver for Frequency-Selective Channels, *IEEE Communications Letters*, 23, pp. 1166-1169, 2019.
- [19] V. Kishore, V. V. Mani, An LED modelled GFDM for optical wireless communications, *AEUE - International Journal of Electronics and Communications*, 101, pp. 5461, 2019.
- [20] Z. Na, J. Lv, M. Zhang, B. A. O. Peng, M. Xiong, M. Guan, GFDM Based Wireless Powered Communication for Cooperative Relay System, *IEEE Access*, 7, pp. 50971-50979, 2019.
- [21] V. Kishore, V. V. Mani, A DC Biased Optical Generalised Frequency Division Multiplexing for IM/DD systems, *Physical Communication*, 33, pp. 1151-122, 2019.
- [22] Y. Wang, D. Wang, J. Ma, On the Performance of Coherent OFDM Systems in Free-Space Optical Communications, *IEEE Photonics Journal*, 7, Open Access, 2015.
- [23] N. A. Mohammed, A. S. El-Wakeel, M. H. Aly, Pointing Error in FSO Link under Different Weather Conditions, *International Journal of Video & Image Processing and Network Security*, 12(1), pp. 6-9, 2012.
- [24] A. Yenilmez, T. Gucluoglu, P. Remlein, Performance of GFDM-maximal ratio transmission over Nakagami-m fading channels, *IEEE International Symposium on Wireless Communication Systems*, pp. 523-527, 2016.
- [25] S. K. Bandari, A. Drosopoulos, V. V. Mani, Exact SER Expressions of GFDM in Nakagami-m and Rician fading channels, *21th European Wireless Conference*, pp. 16, 2015.
- [26] M. P. Ninos, H. E. Nistazakis, G. S. Tombras, On the BER performance of FSO links with multiple receivers and spatial jitter over gamma-gamma or exponential turbulence channels, *Optik*, 138, pp. 269-279, 2017.
- [27] A. Farhang, N. Marchetti, L. E. Doyle, Low-Complexity Modem Design for GFDM, *IEEE Transactions on Signal Processing*, 64(6), pp. 1507-1518, 2016.